

EUROPEAN ORGANIZATION FOR NUCLEAR RESEARCH
Proposal to the ISOLDE and Neutron Time-of-Flight Committee

Single-particle behaviour towards the “island of inversion” -
 $^{28,30}\text{Mg}(d,p)^{29,31}\text{Mg}$ in inverse kinematics

June 1, 2016

D. K. Sharp¹, S. J. Freeman¹, B. B. Back², P. A. Butler³, W. N. Catford⁴,
A. N. Deacon¹, L. P. Gaffney⁵, C. R. Hoffman², R. V. F. Janssens², B. P. Kay²,
Th. Kröll⁶, M. Labiche⁷, G. Lotay⁴, A. Matta⁴, R. D. Page³, R. Raabe⁸ and
D. Steppenbeck⁹

¹*School of Physics and Astronomy, The University of Manchester, Manchester, M13 9PL, UK*

²*Physics Division, Argonne National Laboratory, Argonne, Illinois 60439, USA*

³*Oliver Lodge Laboratory, University of Liverpool, Liverpool, L69 7ZE, UK*

⁴*Department of Physics, University of Surrey, Guildford, GU2 5XH, UK*

⁵*School of Engineering and Computing, University of the West of Scotland, Paisley, PA1 2BE, UK*

⁶*Institut für Kernphysik, Technische Universität Darmstadt, Germany*

⁷*STFC Daresbury Laboratory, Daresbury, Warrington, WA4 4AD, UK*

⁸*KU Leuven, Institut voor Kern- en Stralingsfysica, 3001 Leuven, Belgium*

⁹*RIKEN Nishina Center, 2-1, Hirosawa, Wako, Saitama 351-0198, Japan*

Spokesperson: D. K. Sharp (david.sharp@manchester.ac.uk)

Co-spokesperson: S. J. Freeman (sean.freeman@manchester.ac.uk).

ISOLDE contact: Karl Johnston (karl.johnston@cern.ch)

Abstract: We propose a measurement of the $^{28,30}\text{Mg}(d,p)^{29,31}\text{Mg}$ reactions in inverse kinematics, using the ISOL Solenoidal Spectrometer currently being installed at ISOLDE. The aim of the measurement is to characterise the neutron single-particle trends in the Mg isotones around the island of inversion. The neutron-adding reaction will provide spectroscopic overlaps for the $1d_{3/2}$, $1f_{7/2}$, $2p_{3/2}$ and $2p_{1/2}$ orbitals. The energy differences between these orbitals define the $N = 20$ and 28 shell closures. These data will provide information regarding the evolution of these shell closures, as well as the emergence of the $N = 16$ shell closure, and will be compared to modern shell-model predictions. We request 33 shifts of beam time for this measurement.

Requested shifts: 11 days (33 shifts)

Installation: ISOL Solenoidal Spectrometer



1 Physics case

The region of nuclei around ^{32}Mg ($Z \sim 12$, $N \sim 20$) is known as the “island of inversion” which is so-called because ground states and low-lying excitations originating from intruder configurations have been observed in these nuclei. Intruder configurations are those resulting from the promotion of one or more neutrons across a shell closure, in this case $N = 20$, generating neutron holes in the orbits below the closed shell. This phenomenon was first identified through anomalous ground-state binding energies of Mg, Na and Ne isotopes [2, 3]. The prevalence of intruder orbitals in this region is indicative of a weakening $N = 20$ shell closure as well as increased correlations with unpaired protons. The island of inversion has been characterised through a number of observables using different techniques, including knock-out reactions e.g., Refs. [4, 5], Coulomb excitation e.g., Refs. [6, 7], β NMR e.g., Ref. [8], β decay e.g., Ref. [9] and via γ -ray spectroscopy of excited states e.g., Ref. [10]. The latter measurements were made by a subset of this collaboration.

In the Ne, Na and Al isotopes, there is a “soft” transition to a deformed ground state through transitional nuclei with mixed wave functions. However, the transition is sharper in the Mg isotopes, with ^{30}Mg outside the island with a ground state well described with the absence of cross-shell excitations [11, 12], whilst the low-energy structure of ^{31}Mg suggests there are stronger admixtures of intruder configurations [13]. Measurements of the isobaric analogue resonances in ^{31}Al have also highlighted the drastic change in nuclear structure [14]. Locations of the single-neutron energies and the distribution of neutron strengths have been measured in some of the transitional nuclei leading up to the island of inversion, e.g., ^{25}Ne [15], ^{27}Ne [16], ^{26}Na [17] and ^{35}Si [18], but only very few within this region such as ^{31}Mg [20]. Measurements of the nuclei approaching the island of inversion provide important systematic information of the behaviour of the relevant orbitals. Knock-out reactions have been successful in probing hole-structures and in deciphering initial ground-state overlaps with populated final states; knowledge of the ground-state wave functions is therefore reasonably good. However, knock-out measurements are limited to studying hole states as cross sections to states corresponding to unoccupied orbitals are low. The states of interest in these systems are intruder states from the shell above and so neutron-adding measurements are required.

The difference between the $1d_{3/2}$ and the $1f_{7/2}$ single-particle energies is indicative of the $N = 20$ shell closure, while the energy difference between the $1f_{7/2}$ and $2p_{3/2}$ orbitals is a measure of the $N = 28$ shell gap. The size of these gaps, and how they change, characterises this unique region of the nuclear chart. Along the $N = 17$ isotonic, chain transfer data exist for ^{33}S , ^{31}Si and ^{27}Ne . A reduction in the $N = 20$ shell gap has been observed in ^{27}Ne which is not observed in the other $N = 17$ nuclei. In the absence of data at $Z = 12$, between Ne and Si, it is still an open question as to whether the reduced $N = 20$ shell gap is present or not in Mg. Furthermore, data on this system would help constrain calculations of the single-particle behaviour in the magnesium isotopes towards ^{32}Mg . There have been measurements using knock-out reactions to probe the states in ^{29}Mg [13] following the removal of a neutron from ^{30}Mg . These measurements suggest that there may be single-particle strength in tentative higher-lying $\ell = 1$ and 3 states in ^{29}Mg , populated very weakly in knock out, that could impact on the $2p_{3/2}$ and $1f_{7/2}$

single-particle energies, defining the $N = 20$ and 28 shell gaps. Using neutron-adding transfer reactions, we can ascertain the spin of these ambiguous states and the degree of fragmentation of these single-particle orbitals between ^{31}Si and ^{27}Ne , as well as towards ^{32}Mg .

In this proposal, we will also aim to extract the location of the $2p_{1/2}$ spin-orbit partner for the first time, which provides further information for refining the effective interactions for shell-model calculations. The expected levels, as predicted by shell-model calculations, are shown in Figure 1 for both ^{29}Mg and ^{31}Mg . These have been calculated using the SDPF-MU interaction [19] with $0p - 0h$ configurations only for the positive parity-states and $1p - 1h$ configurations for those of negative parity. The single-particle energies of the $1f$ and $2p$ orbits have been shifted to reproduce the first $7/2^-$ and $3/2^-$ levels in ^{31}Si . The $2p_{1/2}$ strength is predicted to be split between two states, one of which is unbound with a consequently very small γ -decay width.

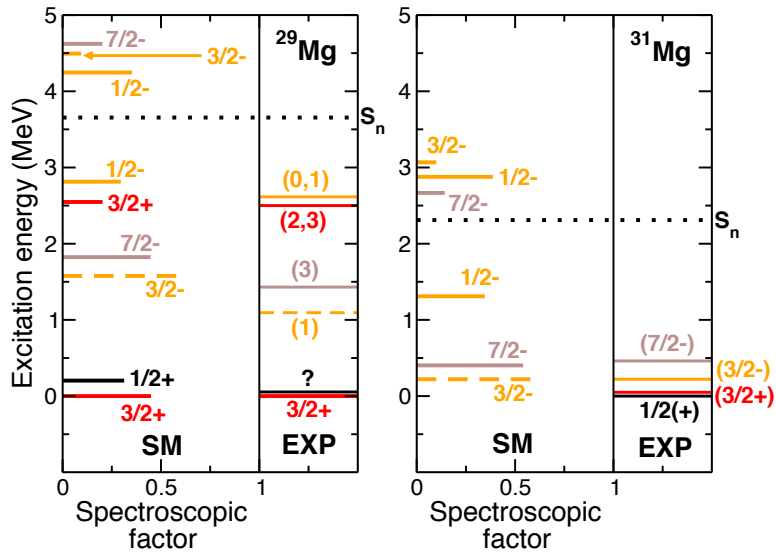


Figure 1: Shell-model calculations for single-neutron states populated in (d,p) reactions using SDPF-MU interaction compared to known low-lying states. Only the experimental energies are presented for comparison. Details of the calculations can be found in the main text. No transfer data exists for states in ^{29}Mg so the experimental levels are those from knock-out measurements [13]. For states in ^{31}Mg , only the ground state and first two excited states have been populated in transfer measurements [20]. The first tentative $7/2^-$ is again from knock-out measurements.

The beam intensities at HIE-ISOLDE are sufficient to probe states in ^{31}Mg , via $^{30}\text{Mg}(d,p)$ in inverse kinematics, allowing us to track these single-neutron excitations into the island of inversion. The $^{30}\text{Mg}(d,p)^{31}\text{Mg}$ reaction has been measured previously at ISOLDE using the T-REX-Miniball set-up [20], where only the first two excited states were identified using a technique that requires γ -proton coincidences at 2.85 MeV/u, relatively low for direct reaction studies. The extracted spectroscopic factor for the $3/2^-$ state at 221 keV of $S = 0.084$ is at odds with the SM predictions shown in Fig. 1. This already suggests that a simple $1p - 1h$ excitation interpretation of the negative parity states

is already too simplistic. Our aim is to make a more robust measurement of the proton yields from neutron transfer to the final states in ^{31}Mg , especially of previously unobserved states that should be strongly populated in this reaction. The previous measurement was affected by long-lived states reducing the γ -ray detection efficiency, which limits the measurement of proton yields for some low-lying states. The resolution of the proton energy spectra is improved by using a solenoid technique such as HELIOS [21, 22] compared to traditional silicon-only techniques. Coincident γ -ray measurements are therefore not required and the extraction of proton yields is *not limited by the lifetime of the state*. The higher beam energies at HIE-ISOLDE allow a measurement at a more ideal energy for transfer reactions, both in terms of larger cross sections and more characteristic angular distributions. Most importantly, at higher energies than was previously accessible, the spectroscopic factors are more robust since a direct mechanism is a better approximation. With the ISOL Solenoidal Spectrometer (see Appendix 1 for a statement on the status of this project), states up to and beyond the neutron separation threshold can be observed as γ -rays are not required to extract the proton yields. This will allow us to probe not just the location of the $f_{7/2}$ and $p_{3/2}$ states, but also the $p_{1/2}$ spin-orbit partner where a significant proportion of the strength is expected to lie above the neutron threshold.

As ^{31}Mg lies just inside the island of inversion, when combined with data on ^{29}Mg , these measurements provide a picture of the evolution of the neutron orbitals in this region of the nuclear chart, mapping out the size of the energy difference between the $1d_{3/2}$ and $1f_{7/2}$ and $2p_{1/2,3/2}$ orbitals. Traditionally, this region has been a challenge for modern shell-model calculations in terms of reproducing the location of the negative parity states. These data will therefore provide a valuable comparison in order to identify the limitations in the current calculations and indicate any contribution from $2p - 2h$ contributions in the ground state, the likely source of any deviation from the shell-model calculations.

2 Experimental details

Reaction and beam energy—We propose to measure single-neutron transfer in inverse kinematics to probe the single-particle structure in neutron rich ^{29}Mg and ^{31}Mg at an incident beam energy of 7.5 MeV/u. At these energies the angular distributions for transfer to final states of differing ℓ are more pronounced and forward peaked, compared to lower energy measurements, such that assignments of the transferred angular momentum are more distinct, see Fig. 2. Though cross sections for the population to some states is higher at somewhat lower beam energies, at these energies the angular coverage of the array is more limited impacting on the ability to make ℓ assignments for the unbound states of interest. Therefore the chosen beam energy is a good compromise between angular coverage and yield. It should be noted that these measurements could be made at 5.5 MeV/u but with somewhat less ideal angular coverage for the unbound states.

ISOL Solenoidal Spectrometer—In inverse kinematics a heavy beam is incident on a light target, in this case deuterated polyethylene (CD_2). The protons from the (d,p) reaction at the forward centre-of-mass angles of interest, are emitted at backwards laboratory angles relative to the incident beam direction. We intend to use the new ISOL Solenoidal

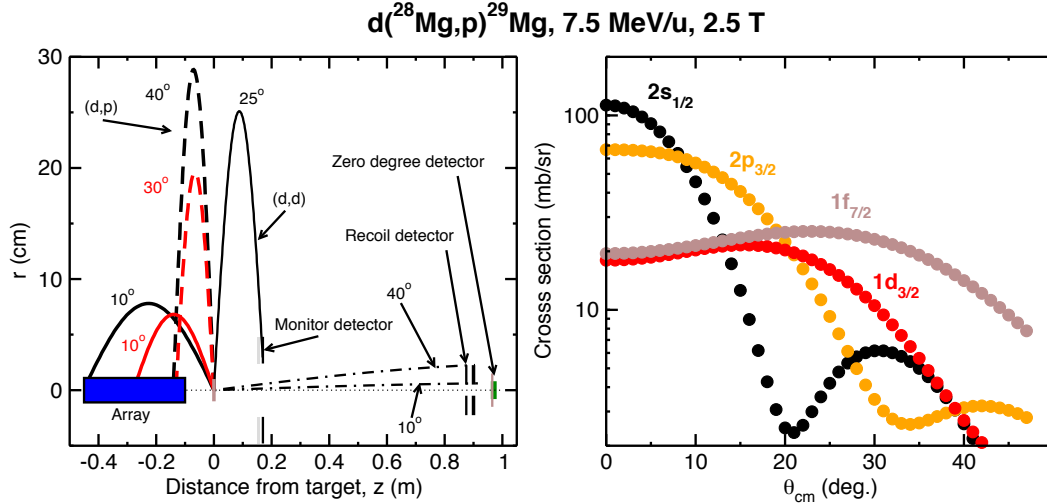


Figure 2: (Left) Proposed experimental set-up within the solenoidal spectrometer. Distances are relative to the target position. For the (d,p) reaction the black line represents protons from population of the ground state whilst the red lines are protons from population of a theoretical state at the neutron separation energy of ^{29}Mg . The hatched lines represent the path of the residual beam-like nuclei. All angles are given in centre-of-mass. See text for detailed description. (Right) Angular distributions in the centre-of-mass calculated for the $2s_{1/2}$ (black), $2p_{3/2}$ (orange), $1d_{3/2}$ (red) and $1f_{7/2}$ (brown).

Spectrometer (ISS) in order to momentum analyse the outgoing protons, measuring energies, and yields of protons populating final states in the residual nuclei of interest. The ISS will be operated in a manner similar to the HELIOS Spectrometer at Argonne National Laboratory (ANL) [21, 22]. For this experiment, the same position-sensitive silicon array and associated electronics from ANL will be used. A Q -value resolution of the Argonne HELIOS array of 70 keV has been achieved at ANL [23]. This collaboration has extensive experience using these detectors. The extracted cross sections and angular distributions will be compared to calculations using the finite-range DWBA code Ptolemy [24], to obtain information on the ℓ of the final states and spectroscopic factors.

A simulation of the $^{30}\text{Mg}(d,p)$ reaction as measured using the ISS is given in Fig. 3. Here an excitation-energy resolution of 100 keV has been assumed with the energies of states taken from previous measurements or from the shell-model predictions. Relative spectroscopic factors are also taken from the shell-model predictions. This resolution is sufficient to extract the proton yields for most final states of interest. The ground and first excited states in both ^{29}Mg and ^{31}Mg , separated by ~ 50 keV, will not be resolved in the excitation energy spectra but with knowledge of the shapes and widths from isolated peaks in the spectrum, and energies from previous work, it will still be possible to still extract yields. Other states are predicted to be well separated in excitation energy.

Experimental set-up—The configuration for the $^{28}\text{Mg}(d,p)$ measurement is shown in Figure 2. The silicon array will be positioned -10 cm from the target as measured to the nearest detector edge, covering a range in z from the target of -10 to -45 cm. The

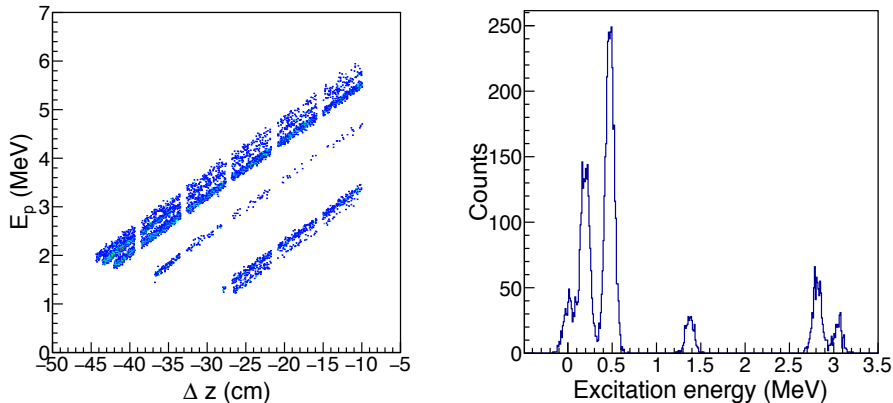


Figure 3: (Left) Plot of proton energy versus the distance from the target at which the proton is detected by the silicon array for the $d(^{30}\text{Mg},p)^{31}\text{Mg}$ reaction. The kinematic lines correspond to protons from different final states in the residual nucleus. A recoil gate has been applied. (Right) Excitation energy spectrum of ^{31}Mg simulated assuming 100 keV resolution. Simulated yields are relative based on the calculated DWBA cross sections and predicted spectroscopic factors.

solenoid field will be set at 2.5 T. With these settings, protons emitted at $10^\circ < \theta_{cm} < 30^\circ$ will be incident on the array for all states up to the neutron separation energy. This range of angles covers the first maxima of the angular distributions for $\ell = 1 - 3$. Spectroscopic factors are best extracted from the peaks of the angular distributions where the assumptions implicit in DWBA are most valid. Elastically-scattered deuterons will be detected in an annular silicon detector positioned at $z = +17$ cm. At a position $z = +90$ cm from the target, an annular ΔE - E telescope will be located. This will detect the recoiling beam-like particles in order to clean the spectra of reactions on beam contaminants and from fusion-evaporation reactions on the carbon in the target. It will also provide a timing reference for the identification of protons in the array, using their cyclotron period as a means of particle identification. A further 7 cm behind the recoil detector, a zero-degree ΔE - E silicon telescope is placed for measuring the unreacted beam and determining its purity. The arrangement is similar for the $^{30}\text{Mg}(d,p)$ measurement.

Beam time request—A beam intensity of 6×10^5 pps of ^{28}Mg has been assumed based on the yield database and an assumption of a proton current of $2\mu\text{A}$ and 5% transmission through HIE-ISOLDE. Contamination of ^{28}Al is expected at the level of 50% [25], so recoil detection is required to separate these contaminants. The array has an efficiency of 50% in the azimuthal angle and 85% in the theta angle. Protons in the angular range $10^\circ < \theta_{cm} < 30^\circ$ will be incident on the array. The CD_2 targets will be $\sim 100 \mu\text{g}/\text{cm}^2$ thick. Cross sections were estimated using the finite-range DWBA code Ptolemy and optical-model parameters of An and Cai [26] and Koning and Delaroche [27] for the deuteron and proton, respectively, assuming a spectroscopic factor of $S = 1$. Under these assumptions we estimate that ~ 800 - 1500 counts per day for the states of interest, namely the $p_{3/2}$, $f_{7/2}$ and $p_{1/2}$ states, will be observed in the whole array. On average there will be ~ 200 counts in each ring of detectors per day. Each ring essentially corresponds to an

angular bin. To obtain a $< 5\%$ statistical error on the spectroscopic factors for a state with $S = 1$ we would require **9 shifts** of beam on target. For the ^{30}Mg we assume 6×10^4 pps again based on the same assumptions from the yield table. This compares well to the 5×10^4 pps observed in IS410 and 1×10^5 pps observed in Ref. [14]. In experiment IS410 a level of ^{30}Al contamination of $\sim 10\%$ was measured, which will be suppressed by the recoil detector. At this rate there will be ~ 80 – 150 counts per day in the whole array for the states of interest. To obtain a $< 10\%$ statistical error on the spectroscopic factors for a state with $S = 1$ we would require **21 shifts** of ^{30}Mg beam on target. We also request a further **3 shifts** of beam on target in order to optimise both the radioactive beams (2 shifts) in to the spectrometer and to account for changes in the set-up between beams (1 shift).

Summary of requested protons: 33 shifts of protons are requested for this measurement. If required this time could be split into **9 shifts** (^{28}Mg) and **21 shifts** (^{30}Mg) plus **2 shifts** for optimisation of each beam.

References

- [1] D. T. Yordanov [Ph.D. Thesis \(Leuven, Belgium\)](#)
- [2] C. Thibault, *et al.*, [Phys. Rev. C **12**, 644 \(1975\)](#).
- [3] E. K. Warburton, J. A. Becker, and B. A. Brown [Phys. Rev. C **41**, 1147 \(1990\)](#).
- [4] A. Gade, *et al.*, [Phys. Rev. Lett. **99**, 072502 \(2007\)](#).
- [5] P. Fallon, *et al.*, [Phys. Rev. C **81**, 041302 \(2010\)](#).
- [6] M. Seidlitz, *et al.*, [Phys. Rev. C **89**, 024309 \(2014\)](#).
- [7] M. Seidlitz, *et al.*, [Phys. Lett. B **700**, 181 \(2011\)](#).
- [8] M. Kowalska, *et al.*, [Eur. Phys. J A **25**, s01, 193 \(2005\)](#).
- [9] F. Maréchal, *et al.*, [Phys. Rev. C **76**, 059902 \(2007\)](#).
- [10] A. N. Deacon, *et al.*, [Phys. Rev. C **82**, 034305 \(2010\)](#).
- [11] B. V. Pritychenko, *et al.*, [Phys. Lett. B **461**, 322 \(1999\)](#).
- [12] O. Niedermaier *et al.*, [Phys. Rev. Lett. **94**, 172501 \(2005\)](#).
- [13] J. R. Terry, *et al.*, [Phys. Rev. C **77**, 014316 \(2008\)](#).
- [14] N. Imai, *et al.*, [Phys. Rev. C **90**, 011302\(R\) \(2014\)](#).
- [15] W. N. Catford, *et al.*, [Phys. Rev. Lett. **104**, 192501 \(2010\)](#).
- [16] S. M. Brown, *et al.*, [Phys. Rev. C **85**, 011302 \(2012\)](#).
- [17] G. L. Wilson, *et al.*, [Journal of Physics: Conference Series **381**, 012097 \(2012\)](#).
- [18] M. G. Burgunder, *et al.*, [Phys. Rev. Lett. **112**, 042502 \(2014\)](#).
- [19] Y. Utsuno (Private communication).
- [20] V. Bildstein. PhD Thesis, Technische Universität München, (2010).
- [21] A. H. Wuosmaa, *et al.*, [Nucl. Instrum. Meth. A, **580**, 1290 \(2007\)](#).
- [22] J. C. Lighthall, *et al.*, [Nucl. Instrum. Meth. A, **622**, 97 \(2010\)](#).
- [23] D. K. Sharp, *et al.*, [Phys. Rev. C **87**, 014312 \(2013\)](#).
- [24] M. H. Macfarlane and S. C. Pieper, ANL-76-11 Rev. 1, ANL Report (1978).
- [25] B. Marsh (Private communication).
- [26] H. An and C. Cai [Phys. Rev. C **73**, 054605 \(2006\)](#).
- [27] A. J. Koning and J. P. Delaroche [Nuc. Phys. A. **713**, 231 \(2003\)](#).

Appendix 1: Status of the solenoidal spectrometer

The £5M UK STFC project, ISOL-SRS, will build two spectrometers, one external and one internal to the Test Storage Ring (TSR), over the period 2015-2019. The external solenoidal spectrometer, ISS (ISOL Solenoidal Spectrometer), will eventually accept cooled beams from the TSR, enabling the energies of final states in two-body reactions to be measured with Q-value energy resolutions of around 20keV FWHM. In order to achieve this, a 50cm six-fold hexagonal DSSD array with 1 mm position resolution in the axial direction and 2 mm in the transverse direction, with individual read-outs, will be constructed. This array will measure the position and energy of light ions emitted from the target as they are deflected through a homogeneous magnetic field on a trajectory that intercepts the detector near the beam axis. This is the “HELIO” technique first developed at ANL ([AH Wuosmaa et al. 2007, NIM A580, 1290](#)). Initial exploitation of HELIOS at Argonne (20+ experiments) has led to 10+ publications, four of which are in Physical Review Letters or Rapid Communications. The studies have been primarily focused on nucleon-transfer reactions with weak radioactive ion beams (RIB).

In light of delays in the approval for the CERN TSR project, CERN management has provided funding to construct a third beam-line dedicated to the external spectrometer that will enable direct HIE-ISOLDE beams to be exploited. The expected energy resolution will be around 45 keV FWHM which is adequate for many experiments that can make use of the large range of accelerated RIB from HIE-ISOLDE. The magnetic field is provided by an ex-MRI magnet purchased by the UK collaboration, which was delivered to CERN in April 2016. While the maximum field in the 1m diameter bore of the magnet is 4T, it is expected that most experiments will use fields in the range 1.5-2.5T. The magnet has field-cancelling coils, and additional Fe shielding will reduce the stray field to levels that satisfy the requirements for both health & safety and for beam acceleration and transport.

Satisfactory readings of the transportation shock-log, coil impedance at room-temperature, etc. suggest that the magnet will cool to liquid helium and be energised without difficulty. It is planned to cool the magnet before the end of 2016 and position it on the end of XT02 (2nd beam line in the ISOLDE hall) at the beginning of 2017. The early-implementation Si array (see below) will be installed and optimised with alpha sources or stable beams during 2017, allowing experiments on ISS to be scheduled in 2018.

While the full DSSD Si array will not be available for experiments until after the second long shutdown at CERN (LS2), the US HELIOS collaboration has offered the use of the position-sensitive Si array currently installed in HELIOS at Argonne ([Lighthall et al. 2010, NIM A 622, 97](#)), together with a heavy-ion recoil detector, for experiments at HIE-ISOLDE. This provides the ISS collaboration with an opportunity to perform (d,p) measurements, before LS2, in particular cases where Q-value energy resolution of around 85 keV is sufficient to resolve the states of interest.

The MRI magnet of ISS will be shared with a second detection setup, the SpecMAT active target of the KU Leuven group. For this project, supported by a €2M ERC grant, the Si array of ISS will be replaced by a gaseous detector surrounded by an array of scintillators. Experiments with this device are also foreseen for 2018, after realisation and commissioning of the setup. The UK and Leuven groups are closely collaborating for the technical and logistical aspects of the use of the magnet.

Note that this major project will strongly benefit from timely entry into CERN's Grey Book, as this would facilitate release of resources to the project, remove obstacles from external collaborators participating in the setting-up phase, and strengthen our applications for further grant funding.

Appendix 2

DESCRIPTION OF THE PROPOSED EXPERIMENT

The experimental setup comprises: The ISOL Solenoidal Spectrometer

Part of the	Availability	Design and manufacturing
(if relevant, name fixed ISOLDE installation: MINIBALL + only CD, MINIBALL + T-REX)	<input type="checkbox"/> Existing	<input type="checkbox"/> To be used without any modification
ISOL Solenoidal Spectrometer	<input type="checkbox"/> Existing	<input type="checkbox"/> To be used without any modification <input type="checkbox"/> To be modified
	<input checked="" type="checkbox"/> New	<input type="checkbox"/> Standard equipment supplied by a manufacturer <input checked="" type="checkbox"/> CERN/collaboration responsible for the design and/or manufacturing

HAZARDS GENERATED BY THE EXPERIMENT (if using fixed installation:) Hazards named in the document relevant for the fixed [MINIBALL + only CD, MINIBALL + T-REX] installation.

Additional hazards:

Hazards			
Thermodynamic and fluidic			
Pressure			
Vacuum			
Temperature	4 K		
Heat transfer			
Thermal properties of materials			
Cryogenic fluid	LHe, ~1650 l, LN ₂ , ~200 l, 1.0 Bar		
Electrical and electromagnetic			
Electricity	0 V, 300 A		
Static electricity			
Magnetic field	2.5 T		
Batteries			
Capacitors			
Ionizing radiation			
Target material	Deuterated polyethylene		
Beam particle type	²⁸ Mg, ³⁰ Mg		
Beam intensity	6×10 ⁵ , 6×10 ⁴		
Beam energy	7.5 Mev/u		
Cooling liquids			

Gases			
Calibration sources:	<input checked="" type="checkbox"/>		
• Open source	<input checked="" type="checkbox"/> (α calibrations source)		
• Sealed source			
• Isotope			
• Activity			
Use of activated material:			
• Description			
• Dose rate on contact and in 10 cm distance			
• Isotope			
• Activity			
Non-ionizing radiation			
Laser			
UV light			
Microwaves (300MHz-30 GHz)			
Radiofrequency (1-300 MHz)			
Chemical			
Toxic			
Harmful			
CMR (carcinogens, mutagens and substances toxic to reproduction)			
Corrosive			
Irritant			
Flammable			
Oxidizing			
Explosiveness			
Asphyxiant	Helium		
Dangerous for the environment			
Mechanical			
Physical impact or mechanical energy (moving parts)			
Mechanical properties (Sharp, rough, slippery)			
Vibration			
Vehicles and Means of Transport			

Noise			
Frequency			
Intensity			
Physical			
Confined spaces			
High workplaces			
Access to high workplaces			
Obstructions in passageways			
Manual handling			
Poor ergonomics			

Hazard identification:

Average electrical power requirements (excluding fixed ISOLDE-installation mentioned above): 5 kW